Authors' accepted manuscript.
Article published in *Fibers and Polymers*, volume 22, pages 1266-1273 (2021)
The final published version is available at https://doi.org/10.1007/s12221-021-9195-x

Accepted in Fibers & Polymers, September 2020

Determination of the Adhesion Between Electrospun Mats through Peel tests

Bouchet Mélusine[1,2,3]; Ajji Abdellah*[3,4]; Lerouge Sophie*[1,2]

[1]Department of Mechanical Engineering, École de technologie supérieure (ÉTS), Montreal, QC, H3C 1K3, Canada

[2]Laboratory of Endovascular Biomaterials (LBeV), Research Centre, Centre Hospitalier de l'Université de Montréal (CRCHUM), Montreal, QC, H2X 0A9, Canada

[3]CREPEC, Department of Chemical Engineering, École Polytechnique de Montréal, Montreal, QC, H3C 3A7, Canada

[4]Institute of Biomedical Engineering, École Polytechnique de Montréal, Montreal, QC, H3C 3A7, Canada

*: Co-corresponding author

Corresponding authors:

Sophie Lerouge, P. Eng., PhD
Laboratory for Endovascular Biomaterials (LBeV)
CHUM Research Center (CHUM)
900 St. Denis Street
Montreal, QC, H2X 0A9, Canada
Tel: +1-514-890-8000 #28821;
Fax: +1-514-412-7785
E-mail: sophie.lerouge@etsmtl.ca

Abdellah Ajji, P. Eng., PhD
CREPEC, Department of Chemical Engineering,
École Polytechnique de Montréal,
PO Box 6079, Station Centre-Ville,
Montréal, QC, H3C 3A7, Canada
Tel: +1-514-340-4711 #3703;
Fax: +1-514-340-4159
E-mail: abdellah.ajji@polymtl.ca

Abstract

Electrospinning is an interesting technique widely used in industry to produce complex fibrous structures with tunable porosity and morphology. Yet, little is known about possible delamination between electrospun layers. In the present work, we studied the adhesion between PCL electrospun mats of similar porosity and investigated the effect of different morphologies, solvents and post-treatment on adhesive strength using a T-peel test. The objective is to establish guiding rules for improving the adhesive strength when fabricating multilayered electrospun systems. The effect of fiber diameter was found to be clearly dominant, large diameter fibers (3.6 μm) showing almost 7-fold increase ($p < 0.0001$) of the adhesive strength compared to smaller ones (0.5 μm), while the use of different solvents for the two layers didn't induce any major change. Heat treatment was also found to improve the adhesive strength. Further study is needed to better understand adhesion mechanisms between electrospun materials. Finally, this T-peel test was found to be an adequate simple tool to test electrospun bilayer materials and evaluate their adhesive strength.

Keywords: Electrospinning, adhesive strength, peel test, multilayer, heat treatment.

1 Introduction

Electrospinning is a fabrication technique of non-woven nano- and micro-fibers mats. It has been largely employed in the last two decades for a wide range of industrial applications such as filters, biosensors and in biomedical engineering. In the latter case, applications such as dressings for wound healing or drug delivery, as well as vascular grafts [1-3] have been developed. In particular, a recent trend is to use electrospinning to fabricate complex designs, including gradient porosity and systems with multiple electrospun layers on top of each other to improve their performance or meet specific design criteria [4-8]. As evoked by Grey et al., who developed an approach by gradient electrospinning to modulate the properties at the boundaries between layers [9], multilayered mats can lead to delamination. Superimposed layers are prone to delaminate over time [10], i.e. the layers detach at the interface, leading to a free space and absence of load transfer to the next layer through the interface. This may impact both the shape and functionality of the product [11, 12]. For example, multilayer electrospun scaffolds are now developed as blood vessel substitutes, to mimic the properties of the native tissue, with each layer mechanically integrated with the bordering others [10]. Lack of cohesiveness of electrospun scaffolds and/or delamination between layers have been observed in several animal studies [10, 13-15], as reported by Lu et al. on bilayer graft after 8 weeks in vivo [14]. Unfortunately, poor results are rarely reported in the literature.

Despite the importance of adhesive strength on the performance of multilayered systems, to the best of our knowledge, little has been reported on the risks of delamination and the adhesive strength between electrospun mats [16-18], most studies being rather focused on the adhesion of

electrospun materials with a matrix to create composites [19-21]. Better understanding of the various parameters which could affect the cohesion between electrospun layers is required. More generally, the study of the delamination between electrospun fibers could provide further understanding of the relationship between the structure and the performance of these widely used electrospun materials.

The objective of the present study was to evaluate peel tests [22] as a simple method to determine the adhesive strength between two electrospun mats and the main factors that influence adhesion. We explored the effect of the fiber diameter, the solvent used for electrospinning the mats and a heat treatment on the adhesive strength of electrospun polycaprolactone (PCL), a biodegradable polymer used in a wide range of applications.

2 Materials and Methods

2.1 Materials and specimen fabrication

Polycaprolactone (PCL, Mn = 80 000) was purchased from Sigma-Aldrich Canada Co., as well as the chemicals, 2,2,2-trifluoroethanol (TFE), chloroform and ethanol. Three different solutions were prepared by dissolving pellets of PCL, as follow: PCL1, 15 wt% into TFE; PCL2, 10 wt% into TFE; PCL3, 15 wt% in a mix of chloroform/ethanol 7:3 (v/v).

PCL bilayer mats were produced on a 6-mm-diameter rotating mandrel using a homemade electrospinning setup. **Table 1** presents the details of the electrospinning parameters for each solution. The electrospinning of the bottom and top layers was spaced out by at least 15 minutes.

The same volume (1 mL) was electrospun for each bottom and top layer. Non-stick aluminium foil pieces were placed on the bottom layer before electrospinning the top layer to allow unbound ends for each layer for subsequent peel tests. Parameters for the electrospinning of PCL3 scaffolds were optimized in order to obtain the same morphology as PCL1 mats. Both layers were electrospun on top of each other to investigate the impact of the solvent nature. PCL2 was produced to study the adhesion between layers presenting different fiber size. Finally, some of the PCL1 and PCL2 bilayer scaffolds were also submitted to a heat treatment in an environmental chamber (Associated Environmental Systems, Acton, MA, U.S.A.) at 65°C for 4 minutes with 20 % humidity, hereafter designated as PCL1HT and PCL2HT, respectively. This treatment was chosen since interfiber bonding was observed through microscopic observation and for its short duration. All samples were extracted from the drum with a scalpel incision along the longitudinal axis, and were cut into rectangular strips having about 20 mm in length for their bonded parts.

2.2 Scaffolds morphology and dimensions

Fibers were observed by scanning electron microscopy (SEM) using a tabletop TM3030Plus instrument (Hitachi, Tokyo, Japan) at 15 kV, after sputter-coating a 20 nm-thickness layer of chromium under vacuum. Images were analyzed using ImageJ (NIH, USA) software. Fiber diameters were calculated based on about 50 different fibers from at least three different specimens for each scaffolds type. The porosity ε of the scaffolds was calculated by the gravimetric method, according to Equation 1 [23].

$$\varepsilon = 1 - \frac{\rho_{mat}}{\rho_{bulk}} \qquad \text{Equation 1}$$

Where ρ_{mat} is the density for each electrospun mat, calculated as the ratio between its mass and volume, and ρ_{bulk} is the bulk density of PCL (1.145 g/cm^3).

The mean pore diameter r was estimated theoretically with a simplification of the model of Eichhorn and Sampson [24], in which it is related to the fiber diameter d and the total porosity ε of the scaffold as indicated in Equation 2 [25].

$$r = -\frac{d}{\ln \varepsilon} \qquad \text{Equation 2}$$

Thicknesses were measured using a Progage Thickness Tester (Thwing-Albert Instrument Company, West Berlin, U.S.A.*).* Mats were sandwiched between two PET films to avoid errors due to compression. The width was obtained from the average of three measures with a digital Vernier caliper (Mitutoyo, Kawasaki, Japan).

SEM analysis was also performed after the peeling tests, in an effort to determine the failure modes [26, 27] and the real contact area between the mats as a function of their morphology.

2.3 Peel test

The T-peel test protocol was established by adapting ASTM D1876 standard [28] to our application, using a mechanical tester Mach-1 v500cst (Biomomentum, Laval, QC, Canada), with a 10 kgf (100 N) load cell. Unbound ends of the test specimen without aluminium foil pieces were clamped in the grips of the testing machine according to **Figure 1,** with an angle of 180° between

both ends. The load was applied at a constant speed of 10 mm/min, until the detachment of the entire length of the specimen. At least six different samples were tested for each bilayer system from three independent experiments.

The adhesive strength *G* between the electrospun layers of each sample is usually calculated with the Equation 3 [29].

$$G = \frac{F}{w}(1 - cos\theta) \qquad \text{Equation 3}$$

Where, F is the average peel force (N), w the width of the sample (m), and Θ the peel angle.

With a T-peel test, the initial peel angle is 180°. This reduces the calculation to the following equation:

$$G = \frac{2F}{w} \qquad \text{Equation 4}$$

The peel angle is assumed to be steady for the entire duration of the test.

2.4 Differential scanning calorimetry

Differential scanning calorimetry (DSC, TA Instruments, New Castle, DE, U.S.A.) was used to characterize the PCL pellets and mats and to determine the melting temperatures to verify if the PCL electrospun fibers presented different properties than bare PCL material. Specimens (weight 3 to 8 mg) were hermetically sealed in an aluminum pan. DSC was performed at a 10°C/min heating rate up to 110°C. The values of the melting temperature were obtained from the

thermograms using the Universal Analysis v4.5 software (TA Instruments, New Castle, DE, U.S.A.).

2.5 Statistical analysis

Data are expressed as the arithmetic mean ± standard deviations. Statistical tests were carried out with GraphPad Prism Software Version 7.0 (San Diego, CA, U.S.A.) using ANOVA with Tukey's post hoc analysis. The normality of data was verified with a Shapiro-Wilk test. P values of less than 0.05 were considered significant.

3 Results

3.1 Mats characterization

All electrospun PCL mats presented random bead-free fiber structures with porosity about 80 % as reported in **Table 2**. Their morphology can be observed on SEM images in **Figure 2** and their structural characteristics are summarized in Table 2. PCL1 and PCL3 had a mean fiber diameter of 3.6 and 3.8 µm, respectively. Microfiber samples were compared to evaluate the impact of different solvent systems used to produce PCL fibers, while PCL2 samples were produced with smaller nanofibers (510 nm in average) to determine the impact of fiber size on the adhesive strength. The standard deviation for the fiber diameter of PCL3 was higher, indicative of more variability in the production of the electrospun PCL fibers with chloroform/ethanol mixture than with TFE. The thickness of samples was 200 ± 59 µm in average.

The effect of the heat treatment on the PCL mats can be seen on **Figure 3AB**, showing that fibers bonded at their contact points (especially visible for PCL1HT). In addition, nanofibers (PCL2HT) seemed to be welded together leading to a merging start. **Figure 3C** shows the DSC curves of PCL granules and the electrospun fibers. It is observed that the melting temperature occurs at 63°C for pellets, while in PCL fibers it decreased to 59.4°C and 58.9°C for PCL1 and PCL2, respectively.

3.2 Adhesive strength

A typical load-extension curve observed during T-peel test is shown on **Figure 4A** First, there is an initial increase of the load until the initiation of the detachment of the two layers, followed by a relatively stable zone where the gradual delamination of both mats occurs until the whole length of the sample is detached or the limit of the machine is reached. The small load variation on the plateau region may be due to local surface alignment of fibers opposing the tensile force. The peel force considered for the calculation of the adhesive strength with Equation 4 corresponds to the average of the load along the plateau.

Results of the T-peel tests for each tested bilayer system are presented in **Figure 4B**. PCL1, PCL2 and PCL3 were tested alone by electrospinning twice the same solution to evaluate their cohesiveness. PCL1 and PCL3 with microfibers reached adhesive strengths of the same order of magnitude, i.e. 65.5 ± 7.9 and 74.4 ± 9.3 mN/mm respectively, whereas PCL2 nanofibers mats displayed significantly lower strength with 9.5 ± 3.1 mN/mm. After a heat treatment of the bilayer PCL1 and PCL2 systems, their adhesive strength significantly increased ($p < 0.0001$) when compared to the values obtained with their initial as-spun bilayer mats. We also evaluated the

adhesive strength of bilayer samples with two different layers and obtained values of 14.4 ± 4.3 and 62.0 ± 16.3 mN/mm, for PCL1 electrospun with PCL2 or PCL3, respectively. The morphology of the peeled mats was observed by SEM. All peeled specimens present similar morphologies compared to before being tested. Defects could be noticed on the surface of fibers from the bilayer system composed only of microfibers, either PCL1 or PCL3 mats (**Figure 5).** No change in the surface was observed when the bilayer peeled sample involved one PCL2 nanofiber mat.

4 Discussion

Little is known about the adhesive strength between electrospun layers despite the wide range of applications in industry. By using a T-peel test we investigated the adhesive strength between different PCL electrospun layers. We selected PCL as it is a widely used polymer in electrospinning studies [2]. However, we believe that the trends observed in our exploratory study for adhesive strength can be extended to other polymeric materials.

The T-peel test described in the ASTM D1876 standard is primarily intended to determine the strength of the adhesive that bonds two laminated panels [28]. We adapted this test for our application to measure the adhesive strength between two materials produced by electrospinning of successive superimposed layers. Differences include smaller sample size and lower peel rate, which was fixed here at 10 mm/min. One limitation of our method is that the angle between the bonded part of the specimen and the direction of tension was not necessarily kept constant at 90° during the test. Bending may have occurred, impacting the concentration of stress as the peel front progressed through the sample [30]. The control over the angle may be done by manually holding

the bonded parts [30], but it might introduce parasitic forces [31]. To overcome these issues, in the future, the bonded parts of the specimen could be held at a 180° angle with one of the peeled arms [30], or a mechanical fixture supporting the unpeeled parts could be designed [31].

We first verified the reproducibility of the T-peel test as a method to determine the adhesive strength between electrospun materials. The coefficient of variation (or relative standard deviation) for the adhesive strength of the microfibers mats (either PCL1 or PCL3) was 12 %, which we estimated to be acceptable to consider the method reproducible [32, 33] due to the variability of the electrospinning process itself [34, 35]. It should be noted that the coefficient of variation however reached 30 % for groups which presented low adhesion values, such as PCL2.

We investigated the effect of the fiber diameter by electrospinning two different mats made with microfibers (PCL1, mean diameter 3.6 μm) and nanofibers (PCL2, mean diameter 510 nm). The adhesive strength between two microfiber mats was almost 7 times greater than that between two nanofiber mats. This result suggests that the fiber diameter had a great impact on adhesion, probably due to the increased area of contact between fibers. This was confirmed by laminating the micro and nanofiber layers together. This led to an adhesive strength only slightly higher than that between nanomats, probably because the contact area remains limited by the nanofibers.

The contact area between two electrospun mats depends both on the fiber diameter and the number of contact points between the two mats, which is very difficult to assess theoretically. In an attempt to quantify it, we took SEM images after peeling, but the quantification of the contact area was not feasible. Indeed, while pieces of residual fibers from the other mat were visible at the surface of microfibers (**Figure 5**), the real contact area could not be determined. It was even more difficult

for nanomats where no defects were observed by SEM on fibers at the interface after peeling. Therefore, our results do not allow to conclude if the adhesive force depends on the mean area for each interfiber contact, the global contact area between the layers or a combination of both. These SEM images suggest that fracture essentially appeared as delamination (fracture between the layers), although some fiber fracture also occurred in the case of the microfibers mats.

In previous works, Wong and others analyzed the adhesion mechanism between electrospun fibers. They determined that adhesion mainly occurs from Van der Waals forces (with the preclusion of capillary bridges between fibers in their evaluation) [16-18, 36]. One study performed on single electrospun fibers showed that the adhesive strength increased with the decreasing fiber diameter [17]. This might look in contradiction with our results. It must however be noted that in their study, the adhesive strength was calculated by dividing the force by the true contact area between the two fibers. In our case, the adhesive strength is calculated by dividing the force during peel test by the sample width. This gives a relative adhesive strength which doesn't take into account the real contact area between the two layers, which depends on the fiber diameter and density at the exact interface.

The impact of solvent nature was studied by comparing the adhesion of PCL mats of similar morphology but prepared with different solvents (TFE for PCL1 and chloroform/ethanol for PCL3). The solvent can impact the adhesion since residual solvent in the fibers can lead to local fusion at junction points between fibers [37, 38]. Solvents with higher vapor pressure at room temperature are expected to evaporate more slowly, leading the solidifying fibers to form stronger bonds with the underlying layer. According to the supplier information, TFE and the

chloroform/ethanol mixture have a vapor pressure of 70 and 116 mmHg respectively (calculated with Raoult's law equation [39]). This might explain the slightly higher adhesion strength observed for PCL3/PCL3 compared to PCL1/PCL1, but the difference was not significantly different ($p = 0.35$).

The adhesive strength was not different when the two layers were electrospun in different solvents (one layer with TFE solution and the other layer with chloroform/ethanol). This might be explained by the fact that PCL can be dissolved with both solvents and their vapor pressure is in the same order of magnitude. However, it might be interesting to determine the impact of using two different materials, electrospun from different solvents, in which they can't dissolve each other.

To improve the adhesion, one method is to fuse the fibers at their junction points. This will increase the number of fibers participating in the adhesion through the thickness of the specimen. It is also known that thermal treatments can increase the tensile properties of electrospun mats [37, 40-42] and affect the crystallinity of the fibers [43]. Usually, the heat treatment is carried out at a temperature between the glass transition and the melting of the material and can last for hours [42, 44]. Another possible way is to heat samples for a short period of time at temperatures above the melting temperature or close to it [41]. This approach was chosen here. The limitation of this approach is that the fibrous network of the structure might be lost with completely molten fibers if the thermal process is not well controlled. Glass transition and melting temperatures of electrospun polymers may differ from up to 10°C from that of the bulk polymer, due to difference in the orientation of molecular chains and the crystallinity [45-49]. Differential scanning calorimetry (DSC) was therefore employed to determine the melting point of electrospun mats and

films of PCL. The glass transition was not studied since it is known to be very far from the temperature of interest here, namely around -60°C for PCL [50]. The melting point of the electrospun fibers was found to be slightly decreased compared to the bulk polymer, from 63 to 59°C (**Figure 3**C). We proposed here a short time for the heat treatment (4 minutes) at a temperature barely above the melting temperature of the bulk (65°C). The heat treatment led to a two-fold increase of the adhesive strength between microfiber mats. The impact on nanofiber mats was found to be even more drastic, with up to a 7-fold increase. The SEM analysis of the mats showed that our specimen kept their fibrous structures. However, their morphology was slightly modified, and the nanofibers seemed to start merging together. Longer heat treatments at lower temperature such as 55°C during 1 hour [40] could be proposed to fuse fiber contact points without the melting effect. Other methods could also be used for increasing adhesion such as the vapor of a proper solvent as post-treatment (like formic acid or dichloromethane)) [51, 52] or blending the electrospun solution with a stickier material [53, 54].

5 Conclusion

The adhesive strength between electrospun mats is still poorly investigated. Here, we proposed simple exploratory trials to give fruitful insights into the understanding of the adhesion properties of electrospun multilayered systems, which can be useful for many industrial applications. We highlighted the impact of the fiber diameter on the adhesive strength which relates to the contact area between fibers at the interface of layers. In order to improve the adhesive strength, if the fiber diameter cannot be increased, it is also possible to use other techniques such as heat treatment. This work is an exploratory study with PCL and further investigations with different materials and

topology (fiber diameter, orientation, porosity) are necessary to better understand all the parameters that may influence adhesion between electrospun materials.

6 Acknowledgements

This research was supported by the Natural Sciences and Engineering Research Council of Canada (NSERC) and the Canadian Institutes of Health Research (CIHR) (CPG 127764). M. Bouchet gratefully acknowledges scholarships from École de technologie supérieure. The authors also thank C. Cerclé (École Polytechnique) for the DSC tests, as well as T. Labonté-Dupuis (ÉTS), M. Gauthier and E. Peigney (École Polytechnique) for their skilled technical support.

References

1. N. Bhardwaj and S. C. Kundu, *Biotechnol. Adv.*, **28**, 325 (2010).
2. J. Xue, T. Wu, Y. Dai, and Y. Xia, *Chem. Rev.*, **119**, 5298 (2019).
3. J. Ding, J. Zhang, J. Li, D. Li, C. Xiao, H. Xiao, H. Yang, X. Zhuang, and X. Chen, *Prog. Polym. Sci.*, **90**, 1 (2019).
4. X. Dong, X. Yuan, L. Wang, J. Liu, A. C. Midgley, Z. Wang, K. Wang, J. Liu, M. Zhu, and D. Kong, *Biomater.*, **181**, 1 (2018).
5. S. A. Shabunin, E. V. Yudin, P. I. Dobrovolskaya, V. E. Zinovyev, V. Zubov, M. E. Ivan'kova, and P. Morganti, *Cosmetics*, **6**, 16 (2019).
6. A. J. Hassiba, M. E. El Zowalaty, T. J. Webster, A. M. Abdullah, G. K. Nasrallah, K. A. Khalil, A. S. Luyt, and A. A. Elzatahry, *Int. J. Nanomed.*, **12**, 2205 (2017).

7. M. J. McClure, D. G. Simpson, and G. L. Bowlin, *J. Mech. Behav. Biomed. Mater.*, **10**, 48 (2012).

8. L. Tan, J. Hu, and H. Zhao, *Mater. Lett.*, **156**, 46 (2015).

9. C. P. Grey, S. T. Newton, G. L. Bowlin, T. W. Haas, and D. G. Simpson, *Biomater.*, **34**, 4993 (2013).

10. I. Woods and T. C. Flanagan, *Expert Rev. Cardiovasc. Ther.*, **12**, 815 (2014).

11. I. S. Raju and T. K. O'Brien, in "Delamination Behaviour of Composites", 1st ed. (S. Sridharan, Ed.), p. 3, Woodhead Publishing, Boca Raton, 2008.

12. G. Amini and A. A. Gharehaghaji, *Int. J. Adhes. Adhes.*, **86**, 40 (2018).

13. Z. Niu, X. Wang, X. Meng, X. Guo, Y. Jiang, Y. Xu, Q. Li, and C. Shen, *Biomed. Mater.*, **14**, 035006 (2019).

14. G. Lu, S. J. Cui, X. Geng, L. Ye, B. Chen, Z. G. Feng, J. Zhang, and Z. Z. Li, *Chin. Med. J.*, **126**, 1310 (2013).

15. M. Gluais, J. Clouet, M. Fusellier, C. Decante, C. Moraru, M. Dutilleul, J. Veziers, J. Lesoeur, D. Dumas, J. Abadie, A. Hamel, E. Bord, S. Y. Chew, J. Guicheux, and C. Le Visage, *Biomater.*, **205**, 81 (2019).

16. F. Montini-Ballarin, T. A. Blackledge, N. L. Capitos Davis, P. M. Frontini, G. A. Abraham, and S.-C. Wong, *Polym. Eng. Sci.*, **53**, 2219 (2013).

17. Q. Shi, K.-T. Wan, S.-C. Wong, P. Chen, and T. A. Blackledge, *Langmuir*, **26**, 14188 (2010).

18. Q. Shi, S. C. Wong, W. Ye, J. Hou, J. Zhao, and J. Yin, *Langmuir*, **28**, 4663 (2012).

19. M. W. Lee, S. An, H. S. Jo, S. S. Yoon, and A. L. Yarin, *ACS Appl. Mater. Interfaces*, **7**, 19555 (2015).

20. ASTM International, "ASTM D882-12, Standard Test Method for Tensile Properties of Thin Plastic Sheeting", ASTM International, West Conshohocken, PA, 2012.

21. J. F. Najem, S.-C. Wong, and G. Ji, *Langmuir*, **30**, 10410 (2014).

22. A. J. Kinloch, C. C. Lau, and J. G. Williams, *Int. J. Fract.*, **66**, 45 (1994).

23. P. R. Cortez Tornello, P. C. Caracciolo, T. R. Cuadrado, and G. A. Abraham, *Mater. Sci. Eng. C*, **41**, 335 (2014).

24. S. J. Eichhorn and W. W. Sampson, *J. R. Soc. Interface*, **2**, 309 (2005).

25. S. Soliman, S. Sant, J. W. Nichol, M. Khabiry, E. Traversa, and A. Khademhosseini, *J. Biomed. Mater. Res. A.*, **96**, 566 (2011).

26. M. Ekrem and A. Avcı, *Compos. Pt. B-Eng.*, **138**, 256 (2018).

27. S. Polat, A. Avcı, and M. Ekrem, *Compos. Struct.*, **194**, 624 (2018).

28. ASTM International, "ASTM D1876-08, Standard Test Method for Peel Resistance of Adhesives (T-Peel Test)", ASTM International, West Conshohocken, PA, 2015.

29. C. Creton and M. Ciccotti, *Rep. Prog. Phys.*, **79**, 046601 (2016).

30. B. A. Morris, in "Science and Technology of Flexible Packaging - Multilayer Films from Resin and Process to End Use", 1st ed. (W. A. Publishing, Ed.), p. 351, Elsevier, United States, 2017.

31. N. Padhye, D. M. Parks, A. H. Slocum, and B. L. Trout, *Rev. Sci. Instrum.*, **87**, 085111 (2016).

32. K. A. Gómez and A. A. Gómez, "Statistical procedures for agricultural research", John Wiley & Sons, New York, 1984.

33. G. F. Reed, F. Lynn, and B. D. Meade, *Clin. Diagn. Lab. Immunol.*, **9**, 1235 (2002).

34. M. Putti, M. Simonet, R. Solberg, and G. W. M. Peters, *Polymer*, **63**, 189 (2015).

35. S. B. Mitchell and J. E. Sanders, *J. Biomed. Mater. Res. A*, **78**, 110 (2006).

36. F. Bobaru, *Model. Simul. Mater. Sc.*, **15**, 397 (2007).

37. I. S. Al-Husaini, A. R. M. Yusoff, W. J. Lau, A. F. Ismail, M. Z. Al-Abri, B. N. Al-Ghafri, and M. D. H. Wirzal, *Sep. Purif. Technol.*, **212**, 205 (2019).

38. J. Chen, L. Sun, and X. Wang, in "ICAFPM 2011: Proceedings of 2011 International Conference on Advanced Fibers and Polymer Materials", p. 545, Chemical Industry Press, Shanghai, 2011.

39. J. B. Ott and J. Boerio-Goates, in "Chemical Thermodynamics: Advanced Applications", 1st ed. (J. B. Ott and J. Boerio-Goates, Eds.), pp. 1, Academic Press, London, 2000.

40. S. K. Tang, J. J. Xie, and J. Xiong, *Gaofenzi Cailiao Kexue Yu Gongcheng/Polym. Mater. Sci. Eng.*, **26**, 66 (2010).

41. M. Kancheva, A. Toncheva, N. Manolova, and I. Rashkov, *Express Polym. Lett.*, **9**, 49 (2015).

42. M. Es-saheb and A. Elzatahry, *Int. J. Polym. Sci.*, **2014**, 1 (2014).

43. C. Ribeiro, V. Sencadas, C. M. Costa, J. L. Gómez Ribelles, and S. Lanceros-Méndez, *Sci. Technol. Adc. Mat.*, **12**, 015001 (2011).

44. M. Miraftab, A. N. Saifullah, and A. Çay, *J. Mater. Sci.*, **50**, 1943 (2014).

45. X. Zong, K. Kim, D. Fang, S. Ran, B. S. Hsiao, and B. Chu, *Polymer*, **43**, 4403 (2002).

46. W. Cui, X. Li, X. Zhu, G. Yu, S. Zhou, and J. Weng, *Biomacromolecules*, **7**, 1623 (2006).

47. F. Liu, R. Guo, M. Shen, S. Wang, and X. Shi, *Macromol. Mater. Eng.*, **294**, 666 (2009).

48. S. Dhakate, B. Singla, M. Uppal, and R. B. Mathur, *Adv. Mater. Lett.*, **1**, 200 (2010).

49. G. K. Arbade, V. Kumar, V. Tripathi, A. Menon, S. Bose, and T. U. Patro, *New J. Chem.*, **43**, 7427 (2019).

50. X. Zhang, X. Peng, and S. W. Zhang, in "Science and Principles of Biodegradable and Bioresorbable Medical Polymers - Materials and Properties", 1st ed. (X. Zhang, Ed.), p. 217, Woodhead Publishing, San Diego, 2017.

51. l. Lei, M. Frey, and T. Green, *J. Eng Fiber. Fabr.*, **1**, 1 (2006).

52. H. Li, C. Zhu, J. Xue, Q. Ke, and Y. Xia, *Macromol. Rapid Commun.*, **38**, 9 (2017).

53. S. Varagnolo, F. Raccanello, M. Pierno, G. Mistura, M. Moffa, L. Persano, and D. Pisignano, *RSC Adv.*, **7**, 5836 (2017).

54. F. Yalcinkaya, *Arab. J. Chem.*, **12**, 5162 (2019).

Tables

Table 1 Process conditions used to produce electrospun bilayer scaffolds

Material	Process parameters						Collector		Ambient	
Polymer	Tip-collector distance (cm)	Voltage (kV)	Flow rate (mL/h)	Needle size (G)	Needle translation (cm)	Translation speed (cm/s)	Ø (mm)	Linear velocity (cm/s)	RH (%)	Temp. (°C)
PCL1	25	15	2	18	11.6	2.2	6	3.8	25-65	20-23
PCL2	25	15	2	18	11.6	2.2	6	3.8	25-65	20-23
PCL3	20	15	4	18	11.6	2.2	6	3.8	20-50	20-23

Table 2 Characteristics of PCL electrospun scaffolds

Materials	Fiber diameter (µm)	Porosity (%)	Pore diameter (µm)
PCL1	3.6 ± 0.4	80.1 ± 1.7	16.2
PCL2	0.5 ± 0.2	79.7 ± 1.5	2.2
PCL3	3.8 ± 1.0	79.8 ± 1.7	16.9

Figure captions

Figure 1. Representation of the T-peel test. (A) Schematisation of the setup. (B) Picture of an ongoing T-peel test.

Figure 2. SEM images of the morphology of different PCL layers (scale bar: 20 µm). (A) PCL1, (B) PCL2, and (C) PCL3.

Figure 3. (A,B) SEM images of the morphology of PCL1 and PCL2 mats after heat treatment (scale bar: 30 µm). (A) PCL1HT and (B) PCL2HT. (C) DSC thermograms of bulk and electrospun PCL.

Figure 4. Representative load-extension curves obtained from T-peel tests using PCL bilayer systems. (B) Adhesive strength of bilayer electrospun PCL scaffolds ($n \geq 6$). On the left side, bilayer systems with 2 similar materials, i.e. twice PCL1, PCL2 or PCL3. The tiled bars represent the adhesive strength after heat treatment of PCL1 or PCL2 bilayer mats, called PCL1HT and PCL2HT, respectively. On the right side, tested bilayer systems with 2 different materials, i.e. PCL1 with PCL2 (3.6 versus 0.5 µm fiber diameter) and PCL1 with PCL3 (TFE vs chloroform/ethanol as solvent). Significant differences are represented as follow: * from PCL1/PCL1, ● from PCL1HT, # from PCL2/PCL2 ($p < 0.0001$).

Figure 5. SEM images of PCL1 mats after a peel test showing defects on microfibers representing pieces of residual fibers from the other microfiber mat of the bilayer system. Scale bars: (A) 20 µm and (B) 10 µm.

Figures

Figure 1:

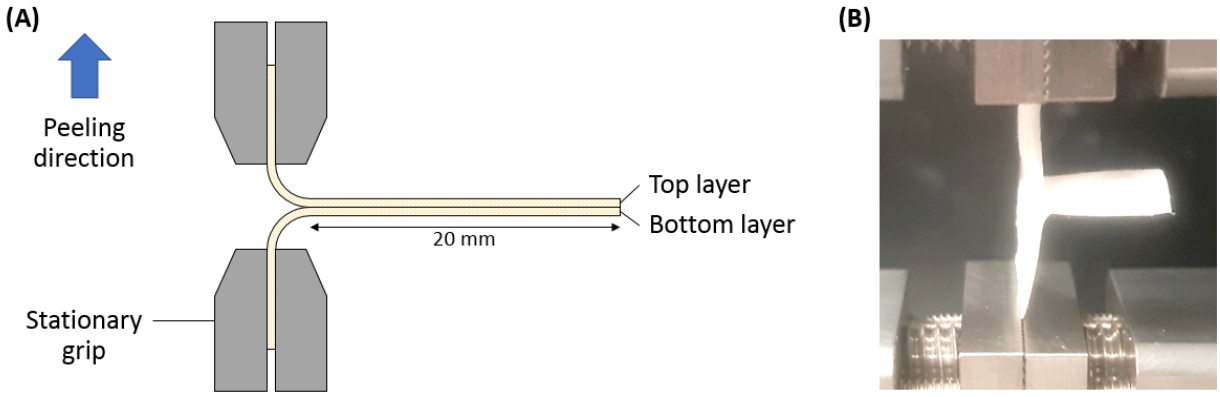

Figure 2:

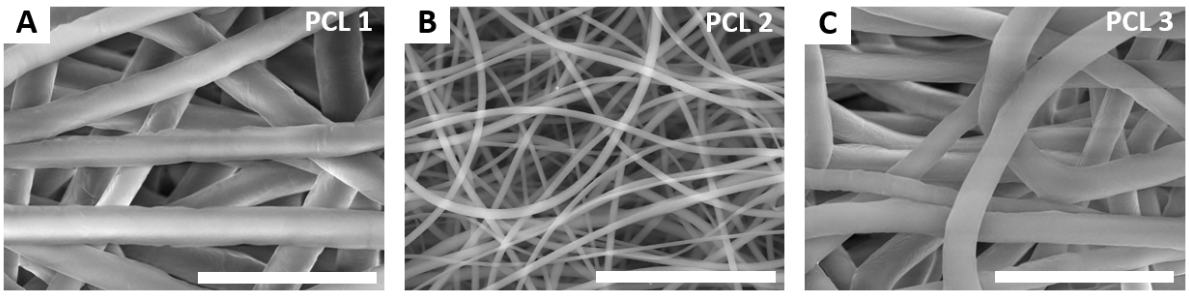

Figure 3:

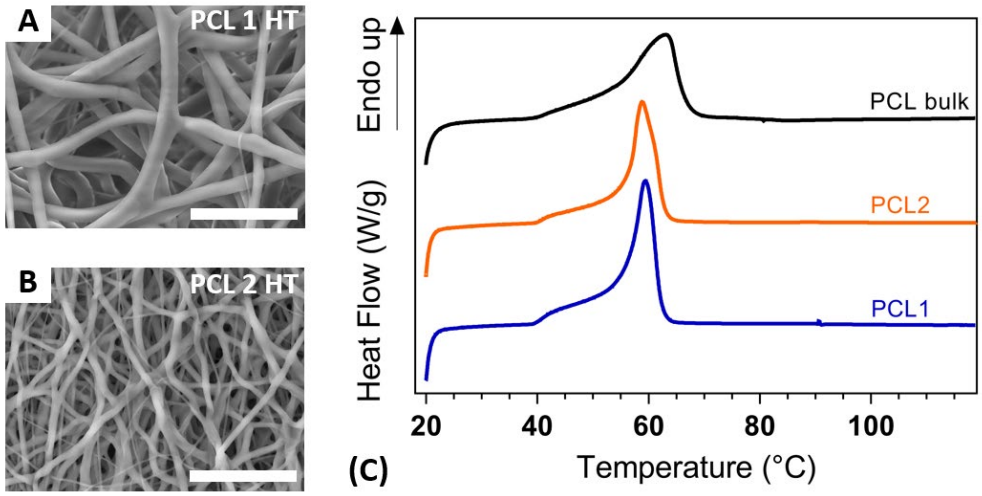

Figure 4:

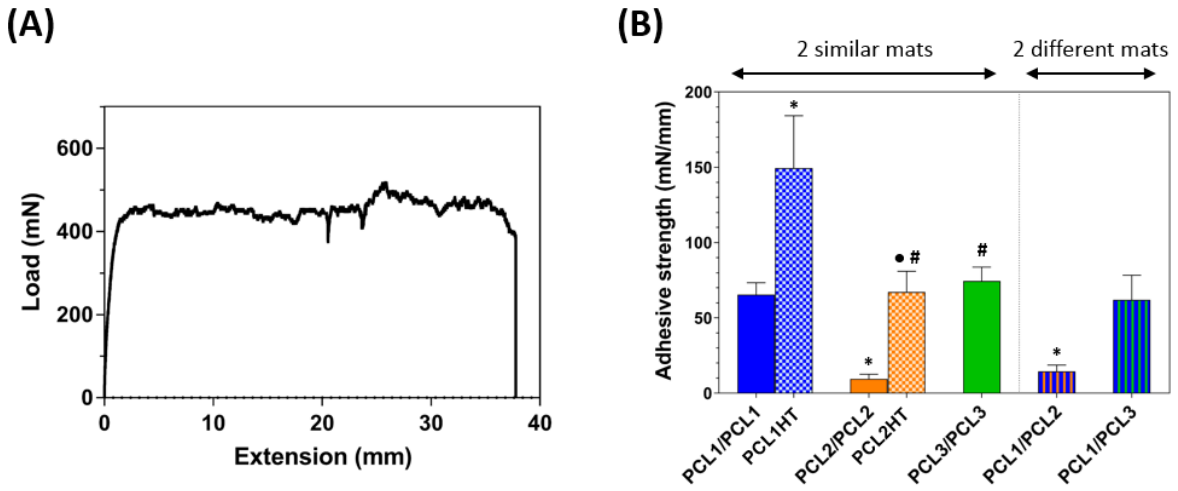

Figure 5: